(15) C. Formoso, *Biochem. Biophys. Res. Commun.*, **50**, 999 (1973).
(16) D. A. Rees, *J. Chem. Soc., B*, 877 (1970).
(17) K. Harata and H. Uedaira, *Nature (London)*, **253**, 190 (1975).
(18) W. Saenger, K. Beyer, and P. C. Manor, *Acta Crystallogr., Sect. B*, **32**, 120 (1976).
(19) A. De Bruyn, M. Anteunis, and G. Verhegge, *Acta Cienc. Indica*, **1**, 83 (1975).
(20) C. W. Haigh and J. M. Williams, *J. Mol. Spectrosc.*, **32**, 398 (1963).
(21) V. S. R. Rao and J. F. Foster, *J. Phys. Chem.*, **67**, 951 (1963).
(22) J. Defaye, D. Gagnaire, D. Horton, and M. Muesser, *Carbohydr. Res.*, **21**, 407 (1972).
(23) D. Gagnaire, D. Horton, and F. R. Taravel, *Carbohydr. Res.*, **27**, 363 (1973).
(24) R. U. Lemieux and J. C. Martin, *Carbohydr. Res.*, **13**, 139 (1970).
(25) M. Sundaralingam, *Biopolymers*, **6**, 189 (1968).
(26) H. M. Berman and S. H. Kim, *Acta. Crystallogr., Sect. B*, **24**, 897 (1968).
(27) D. J. Wood, F. E. Hruska, and K. K. Ogilvie, *Can. J. Chem.*, **52**, 3353 (1974).
(28) C. F. Johnson, Jr., and F. A. Bovey, *J. Chem. Phys.*, **29**, 1012 (1958).
(29) T. Yonemoto, *Can. J. Chem.*, **44**, 223 (1966).
(30) B. V. Cheney, *J. Am. Chem. Soc.*, **90**, 5386 (1968).
(31) E. A. Lewis and L. D. Hansen, *J. Chem. Soc., Perkin Trans. 2*, 2081 (1974).
(32) After submission of our manuscript, we received a preprint from Drs. R. Bergeron and R. Rowan, III (*Bioorg. Chem.*, in press) describing an NMR study of pNP^- binding to α-CD and to β-CD (cycloheptaamylose). They have, as we have, found that pNP^- insertion into α-CD leads to an enhanced shielding of H_3 while H_5 is affected very little. Insertion of pNP^- into β-CD, however, leads to increased shielding for both H_3 and H_5. Their observations are discussed in tems of the extent of guest penetration. Partial penetration into α-CD was evident also in their nuclear Overhauser studies.

A Pulsed NMR Study of Molecular Motion in Solid 6,12,12-Trimethyl-5,6-dihydro-7*H*,12*H*-dibenzo[*c*,*f*][1,5]silazocine

David W. Larsen* and Joyce Y. Corey

Contribution from the Department of Chemistry, University of Missouri–St. Louis, St. Louis, Missouri 63121. *Received July 27, 1976*

Abstract: 6,12,12-Trimethyl-5,6-dihydro-7*H*,12*H*-dibenzo[*c*,*f*][1,5]silazocine was studied in the solid phase by use of pulsed NMR. Values of T_1, $T_{1\rho}$, T_{1D}, and the second moment were measured over the temperature range 85 to 326 K. The compound exhibits four distinct motions in the solid: methyl reorientation (E_A = 2.34 kcal/mol), ring flexing (E_A = 4.14 kcal/mol), molecular reorientation (E_A = 22 kcal/mol), and an unidentified motion ($E_A \geq$ 6.2 kcal/mol). Experimental second moments agree with values calculated from crystallographic data using reduction factors. The possibility of N inversion in the silazocine is discussed.

The rates of conformational change and the activation parameters for various processes have been studied for a large number of systems, both as neat liquids and in solution, by use of high-resolution NMR line shape analysis.[1] The technique applies to values of conformer lifetime, $\tau \sim (\Delta\omega)^{-1}$, where $\Delta\omega$ is the chemical shift between conformers. Since $\Delta\omega$ for organic molecules is not larger than a few ppm, except in unusual instances, and since the temperature region below the freezing point of the liquid may not be investigated by this technique, there are motional processes that cannot be studied, in particular, low activation energy, rapid motions. The scope of molecular motion studies can be increased dramatically by use of the pulsed NMR technique to measure relaxation times (T_1, $T_{1\rho}$, and T_{1D}) and second moments with solid and glass samples. Studies of this type can probe motional frequencies from $\sim 10^3$ to $\sim 10^8$ Hz. The technique is particularly useful for the study of rapid motions, i.e., processes for which activation barriers are less than 10 kcal/mol.

We wish to report an application of the pulsed NMR technique in the study of the molecular motions in the tricyclic system 6,12,12-trimethyl-5,6-dihydro-7*H*,12*H*-dibenzo[*c*,*f*][1,5]silazocine, IA, which contains a central eight-membered ring with silicon and nitrogen heteroatoms.[2] Two idealized conformations are possible for azocine systems, such as I. The twist-boat (flexible) conformer is exhibited in the solid state by ID[3] and the boat-chair (rigid) conformer was reported for IC.[4] Conformational equilibria of solutions of I (X = CH_2; R = Me, H, $CD_2C_6H_5$, $CHMe_2$, CMe_3) have been studied by means of variable temperature NMR and results rationalized in terms of TB ⇄ TB, BC ⇄ BC, and TB ⇄ BC processes.[5] The twist-boat conformer is exhibited by the silazocine, IB, in the solid state as confirmed by a solid state x-ray

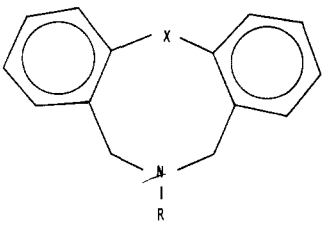

IA X = $SiMe_2$; R = Me
B X = $SiMe_2$; R = t-Bu
C X = CH_2 ; R = Me
D X = CH_2 ; R = t-Bu

study.[2] The solution NMR spectra of I (X = $SiMe_2$; R = Me, CMe_3, CH_2Ph, C_6H_{11}) are identical (except for protons attributed to the exocyclic R group) at room temperature and all exhibit a singlet for the benzyl ($-CH_2-$) ring protons and the singlet persists for both IA and IB down to −60 °C. These observations suggest the presence of a single conformer, the flexible twist-boat conformer, in solution; however, we were unable to measure the value of the activation barrier using high resolution NMR. Pulsed NMR studies on a solid sample of IA have enabled the activation barrier for the ring flexing motion to be determined and have also enabled other molecular motions to be identified and characterized. We presently report the results of the study on solid IA.

Experimental Section

Sample. The compound, IA, was synthesized by the reaction of bis(*o*-bromomethylphenyl)dimethylsilane with methylamine in CCl_4.[2] The solid was recrystallized from heptane, and the sample was placed in a closed glass container for study.

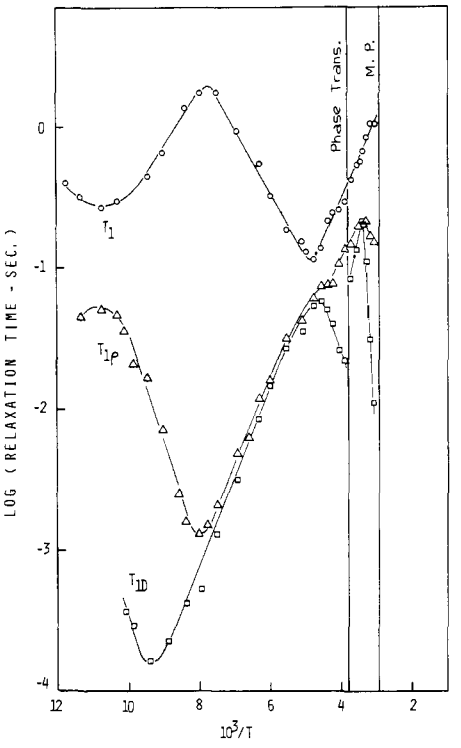

Figure 1. Proton NMR relaxation times of dibenzosilazocine vs. reciprocal temperature.

NMR Measurements. Proton NMR measurements were made using a polaron (Watford, England) high power (2.5 kW) pulsed NMR spectrometer operating at 60 MHz. The rf field is continuously variable up to 60 G, corresponding to a 90° pulse width of 1 μs. The recovery time of the spectrometer following a pulse is 4–5 μs.

The T_1 measurement was done by use of a 90–τ–90 pulse sequence.[6] Values of T_1 were obtained from the plot of log $(M_\infty - M)$ vs. τ, where M is the intensity of the Bloch decay[6] immediately following the second pulse and M_∞ is M when $\tau = \infty$. The values of M were obtained from the trace of a storage oscilloscope; a Tektronix 549, with a writing speed of 2 μs/cm, was used.

The measurement of $T_{1\rho}$ was done by use of a 90° pulse followed immediately by a long "spin locking" pulse of duration τ, which is phase shifted by 90° from the first pulse. Values of $T_{1\rho}$ were obtained from the plot of log M vs. τ, where M is the intensity of the Bloch decay immediately following the long pulse. The Polaron spectrometer is especially stabilized to give a long pulse (up to 10 s) without appreciable droop. For the $T_{1\rho}$ studies, an rf field (H_1) of 28.6 G was used.

The measurement of T_{1D} was done by a three-pulse sequence, 90–τ'–45τ–45, proposed by Jeener,[7] where τ' is less than T_2, and the second pulse is phase shifted by 90° from the first pulse. The third pulse is the "read" pulse and it is in phase with the first pulse. Values of T_{1D} were obtained from the plot of log M vs. τ, where M is the maximum intensity of the signal ("dipolar" signal) following the third pulse.

Values of the second moment[8] were obtained from analysis of the Bloch decay following a single 90° pulse and from analysis of the "solid echo,"[9,10] following a 90–τ–90 pulse sequence, in which τ is slightly longer than the recovery time of the system (~5 μs) and the second pulse is phase shifted by 90° from the first pulse. For the Bloch decay following a 90° pulse, one may write:

$$M \propto \left(1 - \frac{M_2}{2!}t^2 + \frac{M_4}{4!}t^4 - \ldots\right) \qquad (1)$$

but the initial portion of the decay is lost in the recovery time of the system. The "solid echo" is a good approximation to the true Bloch decay with our spectrometer since distortion terms are present in t^4 and higher order, but our recovery time is short enough that the distortion terms are negligible. Furthermore, for the compound IA, the Bloch decay was found to be Gaussian within experimental error.

$$M \propto \exp\left(-\frac{M_2}{2}t^2\right), \qquad (2)$$

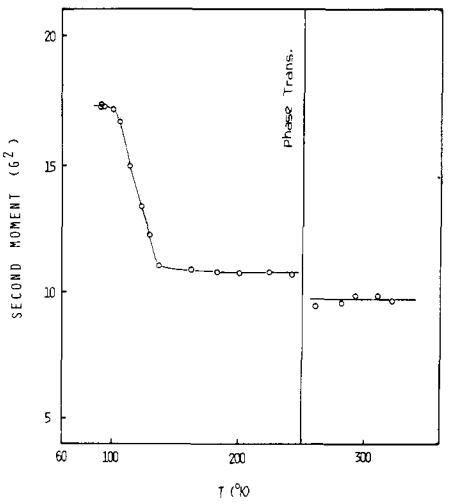

Figure 2. Proton NMR second moments of dibenzosilazocine vs. temperature.

Thus, values of M_2 were obtained from the plot of log M vs. t^2, in a straightforward and rapid manner.

Experimental Results

The experimental relaxation times are presented in Figure 1. Values of T_1, $T_{1\rho}$, and T_{1D} are plotted on a log scale vs. reciprocal temperature; temperature increases from left to right on the abscissa. The experimental second moments are presented in Figure 2. Values of M_2 are plotted vs. temperature. These parameters were studied over the temperature range 85 to 326 K (just below the melting point, 328 K).

The most rapid motion (I) that is observed gives rise to the minimum in T_1 at $10^3/T = 10.7$ (93 K). The Zeeman relaxation time, T_1, is affected to a good approximation only by a motion with frequency near the Larmor frequency (60 MHz) and can be described by the Bloembergen, Purcell, and Pound (BPP) theory.[11] This is a "weak collision" theory and it predicts:

$$1/T_1 = C_1 J(\omega_0) + C_2 J(2\omega_0) \qquad (3)$$

where $\omega_0 = \gamma H_0$ is the Larmor frequency in the static magnetic field H_0, C_1 and C_2 are constants, and $J(\omega)$ is the spectral density function for the motion. For a random motion, characterized by an exponential correlation function, one may write:

$$J(\omega) = \tau_c/(1 + \omega^2\tau_c^2) \qquad (4)$$

where τ_c is the correlation time of the motion, which is usually assumed to follow an Arrhenius expression:

$$\tau_c = \tau_0 \exp(E_A/kT), \qquad (5)$$

Equation 3 can be rewritten for solid samples:

$$\frac{1}{T_1} = \frac{2}{3}\gamma^2 M_{2\text{mod}}\left[\frac{\tau_c}{1 + \omega_0^2\tau_c^2} + \frac{4\tau_c}{1 + 4\omega_0^2\tau_c^2}\right] \qquad (6)$$

where γ is the gyromagnetic ratio and:

$$M_{2\text{mod}} = M_{2(\text{low})} - M_{2(\text{high})} \qquad (7)$$

$M_{2\text{mod}}$ is the portion of M_2 which is modulated by the motion, $M_{2(\text{low})}$ is the limiting value of M_2 when the motion is too slow to affect the line, and $M_{2(\text{high})}$ is the limiting value of M_2 when the motion is sufficiently rapid to cause the line to be motionally narrowed. Equation 6 predicts a minimum value for T_1 when:

$$\omega_0\tau_c = \nu_0/\nu_c = 0.616 \qquad (8)$$

where $\nu_c = (2\pi\tau_c)^{-1}$ is the correlation frequency in Hz and $\nu_0 = \omega_0/2\pi$ is the Larmor frequency in Hz. Thus, at the minimum in T_1 at 93 K, motion I is characterized by $\nu_c = 9.72 \times 10^7$ Hz. Equations 5 and 6 indicate that an estimate of E_A can be obtained from the gradient on either side of the minimum. On the high temperature side of the T_1 minimum ($10^3/T$ between 8.0 and 9.5), there is a small contribution to the observed T_1 ($T_{1(obsd)}$) from an additional motion T_{1A}, which must be subtracted according to:

$$\frac{1}{T_1} = \frac{1}{T_{1(obsd)}} - \frac{1}{T_{1A}} \tag{9}$$

The gradient of $T_{1(obsd)}$ corresponds to $E_A \approx 1.8$ kcal/mol, but the gradient of T_1 from eq 9 gives $E_A = 2.34$ kcal/mol. Thus motion I is characterized by $\tau_c = (7.6 \times 10^{-12}) \exp(2.34 \times 10^3/RT)$. This motion is attributed to reorientation of the methyl groups about their respective C_3 axes. This motion will be discussed further below.

The next most rapid motion (II) to be observed gives rise to several effects. In Figure 1, the T_1 minimum at $10^3/T = 4.85$ (206 K), the $T_{1\rho}$ minimum at 7.81 (128 K), and the minimum in T_{1D} at 9.35 (107 K) are all attributed to this motion; in addition, the break in M_2 between 100 and 120 K in Figure 2 is also attributed to this motion. The Zeeman relaxation time, T_1, can be treated as described above. $T_{1\rho}$ is the time characterizing the relaxation of "Zeeman" order in the rotating frame. A "weak collision" BPP type theory[12] predicts:

$$\frac{1}{T_{1\rho}} = C_{1\rho}J(\omega_0) + C_{2\rho}J(2\omega_0) + C_{3\rho}J(2\omega_\rho) \tag{10}$$

where $\omega_\rho = \gamma H_\rho$ is the resonance frequency in the effective field in the rotating frame and $C_{1\rho}$, $C_{2\rho}$, and $C_{3\rho}$ are constants. In this case $H_\rho = H_1$. Equation 10 can be rewritten for solid samples:

$$\frac{1}{T_{1\rho}} = \gamma^2 M_{2\mathrm{mod}} \left[\frac{\tau_c}{1 + 4\omega_\rho^2\tau_c^2} + \frac{5\tau_c/3}{1 + \omega_0^2\tau_c^2} + \frac{2\tau_c/3}{1 + 4\omega_0^2\tau_c^2} \right] \tag{11}$$

which reduces to:

$$\frac{1}{T_{1\rho}} = \gamma^2 M_{2\mathrm{mod}} \frac{\tau_c}{1 + 4\omega_\rho^2\tau_c^2} \tag{12}$$

in the vicinity of the $T_{1\rho}$ minimum, which occurs when $\nu_c = 2\nu_\rho = 2\gamma H_1 = 2.45 \times 10^5$ Hz. T_{1D} is the time characterizing the relaxation of "dipolar" order.[13] Theories for this process are known for two limiting cases, (a) the "weak collision" case in which $\tau_c \ll T_2(\mathrm{rl})$, the spin-spin relaxation time of the rigid lattice, and (b) the "strong collision" case in which $\tau_c \gg T_2(\mathrm{rl})$. The former case applies roughly to the high temperature arm of the T_{1D} minimum and the latter case applies roughly to the low temperature arm. The dipolar relaxation rate calculated from the "weak collision" theory is:

$$\frac{1}{T_{1D}} = C_{1D}J(\omega_0) + C_{2D}J(2\omega_0) + C_{3D}J(0) \tag{13}$$

and that calculated from the "strong collision" theory[14] is:

$$1/T_{1D} = 2(1 - p)/\tau_c \tag{14}$$

where p is a geometrical parameter which takes into account any correlation in the local fields before and after collision. A theory for the T_{1D} minimum is unknown; however, it has been suggested[15] that the two cases can be joined by a heuristic approach giving:

$$\frac{1}{T_{1D}} = C_{1D}J(\omega_0) + C_{2D}J(2\omega_0) + C'_{3D}J(\omega_L) \tag{15}$$

where $\omega_L \approx \gamma H_L$ is the resonance frequency in the local (dipolar) field. Thus, a T_{1D} minimum is predicted when $\omega_L\tau_c \sim 1$, in this case when $\nu_c \sim 10^4$ Hz.

The second moment of the NMR line is defined[8] by:

$$M_2 = \frac{\gamma^2 \int (\omega - \omega_{max})^2 g(\omega)\, d\omega}{\int g(\omega)\, d\omega} \tag{16}$$

where the integral is taken over the central portion of the NMR line of shape $g(\omega)$. In regions in which M_2, and thus the line width δH, are temperature dependent, the correlation frequency can be estimated[16] from:

$$\nu_c = \alpha\gamma\delta H \left[\tan \frac{\pi}{2} \left\{ \frac{(\delta H)^2 - (\delta H)^2_{high}}{(\delta H)^2_{low} - (\delta H)^2_{high}} \right\} \right]^{-1} \tag{17}$$

where $(\delta H)_{low}$ is the line width when the motion is too slow to affect the line (low temperature limit), $(\delta H)_{high}$ is the line width when the motion is sufficiently rapid to cause the line to be motionally narrowed (high temperature limit), and α is a constant of order unity.[17] As stated above, we have found the lines to be Gaussian in this case; thus, $(\delta H)^2 = 4M_2$ and eq 17 becomes:

$$\nu_c = 2\alpha\gamma M_2^{1/2} \left[\tan \frac{\pi}{2} \left\{ \frac{M_2 - M_{2(high)}}{M_{2(low)} - M_{2(high)}} \right\} \right]^{-1} \tag{18}$$

The relationship between relaxation time minima and the second moment transition is clearly illustrated by motion II. The T_{1D} minimum at 107 K corresponds to the onset of the transition in M_2; the $T_{1\rho}$ minimum at 128 K corresponds roughly to the middle of the M_2 transition;[18] the T_1 minimum at 206 K occurs in the flat region[19] of $M_2 = M_{2(high)}$, well beyond the transition.

Correlation frequencies for motion II were obtained from the minima in T_1, $T_{1\rho}$, and T_{1D} by use of the above expressions, and these are presented in Figure 3. The large uncertainty in ν_c from the T_{1D} minimum is a consequence of the uncertainty in the theory. Also shown in Figure 3 is one point obtained from the observed value of $T_{1\rho}$ at $10^3/T = 10.0$, using the Slichter-Ailion (SA) analysis,[14] in the slow motion limit:

$$\frac{1}{T_{1\rho}} = \frac{2(1 - p)H_L^2}{H_1^2 + H_L^2} \left(\frac{1}{\tau_c}\right) \tag{19}$$

In this expression, p is a quantity similar to that in eq 14, $H_1 = 28.6$ G, and $H_L^2 = \frac{1}{3}M_2$,[20] which we assume to be $\frac{1}{3} \cdot M_{2\mathrm{mod}}$. There is an uncertainty in values of τ_c calculated from this expression due to uncertainty in the value of p.[21] A range of ν_c values was calculated using a range of p values in eq 19, as shown in Figure 3. This point will be discussed below. From Figure 3, it can be seen that ν_c values covering about five orders of magnitude are obtained from this motion II.[22] The activation energy for this motion, from Figure 3, is $E_A = 4.14$ kcal/mol. The motion is characterized by: $\tau_c = (6.7 \times 10^{-14}) \exp(4.14 \times 10^3/RT)$. Estimates of E_A can also be made from the gradients on either side of minima, after correction is made from contributions from other motions. This procedure is in general not as accurate as that used in Figure 3, and lower estimates of E_A are obtained. In this case, values ranging from 3.1 to 3.7 kcal/mol are obtained from the gradients.

Correlation frequencies for motion II were also obtained from the M_2 transition of Figure 2 by use of eq 18. Absolute values of ν_c cannot be obtained without a knowledge of α. Thus values of $\log(\nu_c/\alpha)$ vs. $10^3/T$ are plotted in Figure 4. This plot gives a value of $E_A = 3.9$ kcal/mol, with considerable experimental scatter. Comparison of Figures 3 and 4 shows that $\alpha \sim 1$ for this motion. We assign motion II to flexing of the C-N-C segment in the central ring; this motion will be discussed below.

The third motion (III) to be observed gives rise to the negative slope in T_{1D} for $10^3/T$ between 3.8 and 4.6. This indicates

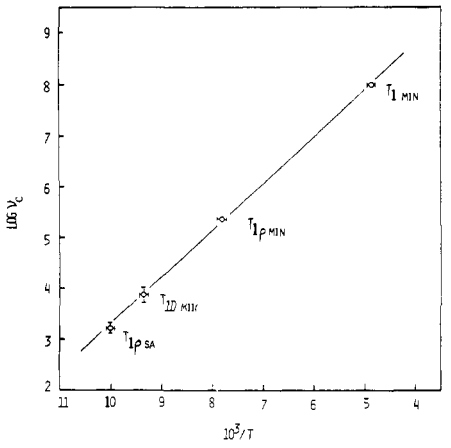

Figure 3. Correlation frequencies of dibenzosilazocine obtained from relaxation time data vs. reciprocal temperature.

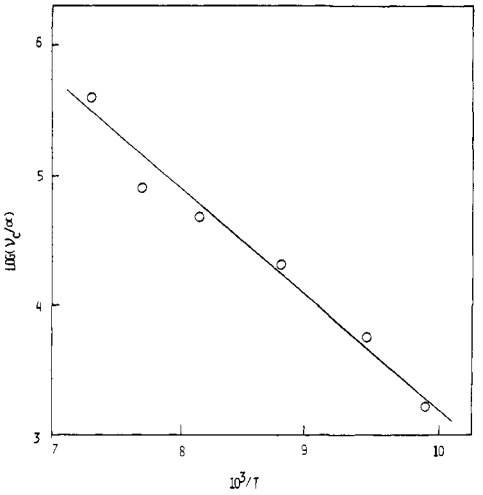

Figure 4. Correlation frequencies of dibenzosilazocine obtained from second moment data vs. reciprocal temperature.

the onset of a new motion with an approximate $E_A \sim 6.2$ kcal/mol, after correction is made for the contribution to the observed T_{1D} in this temperature range from motion II according to an equation similar to eq 9. A discontinuity is observed in T_{1D} at $10^3/T = 3.8$ (−10 °C) and the slope of T_{1D} is positive for temperatures just above the discontinuity. Figure 2 also shows a discontinuity at the same temperature. This discontinuity is attributed to a low enthalpy phase change. Studies made on a differential scanning calorimeter[23] show an extremely small peak at ~6 °C. Thus, the phase change is probably a minor modification in the structure, which gives rise to a slightly lower value of M_2, about 1 G^2 lower. The motion (III) controlling T_{1D} in the vicinity of the discontinuity is probably associated in some way with the phase change, and as the compound undergoes the phase change, the time scale of this motion is changed discontinuously. T_1 and $T_{1\rho}$ are still controlled by the flexing motion (II) in this temperature region. Since there are no minima in relaxation times or transitions in M_2 associated with motion III, it cannot be characterized further, and thus a definite assignment cannot be made. However, it is possible that the motion could involve inversion at the N in the central ring. This point will be discussed below.

The fourth motion (IV) to be detected results in a negative slope in T_{1D} for $10^3/T$ between 3.0 and 3.4, just below the melting point. This motion has an activation energy $E_A \approx 22$ kcal/mol and it is probably reorientation of the entire molecular structure in a more or less isotropic manner. This is presumably the onset of motion which leads to melting. This type of motion has been observed for benzene and other molecules.[24] It is possible that this motion may involve to some extent a conformational change of the central ring from twist-boat (TB) to boat-chair (BC) form.[5]

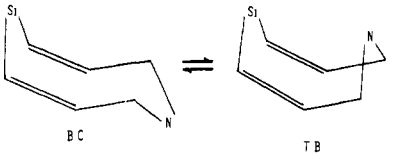

A summary of the experimental parameters for motions I–IV is presented in Table I.

Table I. Observed Motions for Dibenzosilazocine

Motion	Tentative assignment	E_A, kcal/mol	τ_0, s
I	CH_3 rot.	2.34[a]	7.6×10^{-12}
II	C–N–C flex (N inversion)	4.14[b]	6.7×10^{-14}
III		6.2[c]	
IV	Molecular rot. (TB ⇄ BC)	22[d]	

[a] Estimated experimental error ±0.3 kcal/mol. [b] Estimated experimental error ±0.1 kcal/mol. [c] Estimated experimental error ±0.5 kcal/mol. [d] Estimated experimental error ±1 kcal/mol.

Discussion

Second moments may be calculated by use of the theory of Van Vleck,[25] which predicts, for a rigid polycrystalline sample:

$$M_2(\text{rl}) = \frac{715.9}{n} \sum_{j>k} r_{jk}^{-6} \qquad (20)$$

where M_2(rl) is the "rigid lattice" value of M_2 in G^2, n is the number of protons in the sample, and r_{jk} is the distance between protons j and k in Å. The sum is taken over all proton pairs in the sample. This expression omits contributions from ^{13}C, ^{14}N, and ^{29}Si, which are negligible in this case. For convenience, M_2 can be separated into intramolecular and intermolecular parts:

$$M_2 = M_{2\text{intra}} + M_{2\text{inter}} \qquad (21)$$

in which $M_{2\text{intra}}$ is evaluated for a single molecule and $M_{2\text{inter}}$ is usually evaluated for one or two nearest neighbors, since r_{jk}^{-6} falls off rapidly with distance.

We have evaluated $M_{2\text{intra}}$ from the x-ray structure of *N-tert*-butylsilazocine analogue,[3] with replacement of a methyl group for the *tert*-butyl group and use of 1.00 Å C–H bond distances. The bond angles at the *N*-methyl group were allowed to vary until the repulsions were minimized; the calculation was done by use of a computer. Values of r_{jk} were then calculated from this "rigid lattice" structure, from which $M_{2\text{intra}}$ was calculated by use of eq 20. Inspection of the contributions from all the 210 proton pairs shows that $M_{2\text{intra}}$ can be broken up into intragroup and intergroup contributions, with the latter arising only from relatively close groups. These results are illustrated in Figure 5, in which numerical values are in G^2, and the value of $M_{2\text{intra}}$ is simply the sum of all terms, 36.1 G^2. The value of $M_{2\text{inter}}$ cannot be calculated without knowledge of the crystal structure, which has not been determined for the molecule. An approximate value of 6 G^2 has been suggested for substances containing many protons;[26,27] however, calculations done by us on similar systems[28] indicate that the value of $M_{2\text{inter}}$ for this molecule is about 4 G^2. Thus we estimate M_2(rl) = 40.1 ± 2 G^2. Examination of Figure 2 shows that the

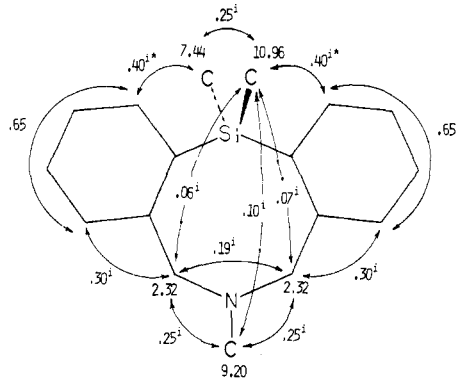

Figure 5. Calculated intragroup and intergroup contributions to the rigid lattice second moment of dibenzosilazocine: i designates an intergroup contribution; * designates interaction of α ring proton with both Si-methyl groups.

rigid lattice value of M_2 is not observed at the lowest temperature attained in this study, and thus the NMR line is narrowed by motion at 90 K. There is a small flat region just below the M_2 transition in Figure 2, and this can be used for comparison with M_2 values calculated assuming a certain motion, in this case reorientation of methyl groups about their C_3 axes. The small flat region corresponds to $M_{2(\text{high})} = M_{2(\text{Me rot.})}$. The value of M_2 for methyls rapidly reorienting can be calculated by use of a reduction factor.[27] If it is assumed that the methyl groups are randomly reorienting at a rapid rate about their respective C_3 axes, the methyl contributions to M_2 are reduced to exactly ¼ its rigid lattice value.[27] The appropriate intergroup contributions are also reduced substantially, and for simplicity, we assume the same factor ¼, since this contribution is relatively small. We assume a reduction[29] in $M_{2\text{inter}}$ to 2.5 G^2, which gives a total value $M_{2(\text{Me rot.})} = 16.6 \pm 2$ G^2. This is in good agreement with the observed value 17.4 G^2.

The M_2 transition which we attribute to flexing of the C-N-C group should be characterized by $M_{2(\text{high})} = M_{2(\text{flex})}$, which corresponds to the flat portion of Figure 2 between 160 and 250 K. This value is relatively difficult to calculate since it requires a knowledge of the details of the motion. However, an approximate calculation can be done for an assumed motion model. Examination of Dreiding models indicates that the flexing of the central ring at the C-N-C group modulates the angle of the CH_2 interproton vector, the axis of CH_3 reorientation, and various intergroup interactions (both angles and distances). In fact, the motion probably modulates all interactions to a greater or lesser extent, but we will consider only the major contributions. To proceed with the calculation, we must first consider the theory of Van Vleck in more detail. The basic expression predicts:

$$M_2 \propto \sum_{j>k} M_{jk}^2$$

in which:

$$M_{jk} = (3\cos^2\theta_{jk} - 1)r_{jk}^{-3} \qquad (22)$$

and θ_{jk} is the angle between proton pair vector r_{jk} and the applied field H_0. Molecular motions such as reorientation of the CH_3 axis and CH_2 rocking affect only θ_{jk} for the intragroup contribution, but they affect both θ_{jk} and r_{jk} for the intergroup contribution. For the CH_2 rocking motion, we will consider a two state model with motion through an angle of 90°. The expressions of Andrew and Eades[30] may be solved for this motion to give a factor $[1 + 3\cos^2\theta]/4$ where θ is the angle of the motion. This factor is ¼ for $\theta = 90°$. We assume that the N-CH_3 bond moves through 90°, which also gives a factor ¼ for the N-CH_3 contribution to M_2. We also assume that the intermolecular contribution is reduced to 2 G^2. This

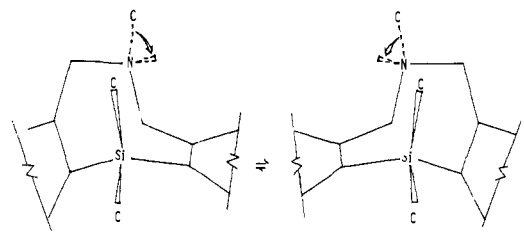

Figure 6. Conformations for the central ring flexing of dibenzosilazocine. N inversion is shown in each conformer.

gives $M_{2(\text{flex})} = 10.1 \pm 2$ G^2, which is in good agreement with the observed value, 10.7 G^2.

The use of eq 19 to calculate τ_c in the "strong collision" limit requires a knowledge of p. The value of p may be calculated from expressions given by Slichter and Ailion[14] if a model for the ring flexing motion is assumed. As stated above, molecular models indicate that when the ring jumps from one flexible conformer to the other, each methylene interproton vector changes by about 90°. Thus the contribution to $T_{1\rho}$ from methylene protons during ring flexing can be calculated from a two-state model characterized by angles ϕ_0 and $\phi_0 + \pi/2$. There will also be an intramolecular contribution to $T_{1\rho}$ from other proton pairs and an intermolecular contribution. Fortunately, the contribution to $M_{2\text{mod}}$ for this motion from methylene protons is much larger than all other contributions, and thus we consider only methylene protons. Following Slichter and Ailion,[14] we obtain:

$$p = \frac{2(1 - 3\sin^2\theta_H + 9\sin^4\theta_H \sin^2\phi_0\cos^2\phi_0)}{2 - 6\sin^2\theta_H + 9\sin^4\theta_H(\sin^4\phi_0 + \cos^4\phi_0)} \qquad (23)$$

where θ_H is the angle between the rotation axis and the strong field H_0, and ϕ_0 is the azimuthal angle for the orientation of the interproton pair vector.[14] A numerical powder average over θ_H and ϕ_0 yields $p = -0.16$. We have calculated ν_c values from eq 19 assuming $0 \geq p \geq -0.32$ as shown in Figure 3. It should be pointed out that the "weak collision" limit result, eq 12, yields essentially the same numerical result.

The question of pyramidal inversion at N for this compound is an interesting one. Activation barriers for N inversion are strongly dependent on molecular structure.[31-35] However, a barrier ≥6 kcal/mol appears to be reasonable for N inversion in this case. If we consider this motion to occur along with ring flexing, there would be an additional reduction in M_2 by about 0.6 G^2, using the above described reduction factor. This gives M_2 (flex + N inv.) = 9.5 ± 2 G^2, which is also consistent with the observed value within experimental error; thus, no definite conclusion can be drawn as to whether motion II is ring flexing or ring flexing + N inversion. Some insight into the nature of motion II is gained by examination of Dreiding models, which suggests that the flex motion conformers are as illustrated in Figure 6. N inversion can then occur only in either ring flex conformer but not during the flexing process, and the flexing motion can only occur when the *N*-methyl is equatorial. Thus the flex motion and the N inversion must be concerted in some sense. It should be noted here that the observed barrier for methyl reorientation (2.3 kcal/mol) suggests that the steric hindrance for the methyls is not unusually large.[36]

It is also possible that motion III could be N inversion, since the observed change in M_2 for the phase transition is ~1 G^2. However, a phase transition will certainly affect $M_{2\text{inter}}$ and since this factor cannot be calculated for an uncharacterized phase transition, no conclusion can be drawn as to this possible assignment for motion III.

Finally, it does not appear that N inversion without ring flexing can account for the M_2 transition in Figure 2, since this would correspond to $M_{2(\text{N inv.})} = 14.4 \pm 2$ G^2 (using the above

Table II. Observed and Calculated Second Moments (G^2)

Structure	M_{2intra}	M_{2inter}	M_{2calcd}	M_{2obsd}
Rigid	36.1	4	40.1 ± 2	
Me rot.	14.1	2.5	16.6 ± 2	17.4
N inv.	12.4	2	14.4 ± 2	
Flex	8.1	2	10.1 ± 2	10.7
Flex + N inv	7.8	1.7	9.5 ± 2	10.7

treatment), which is not consistent with the experimental observation. These results are summarized in Table II.

Acknowledgments. We wish to thank Dr. H. K. Yuen of the Monsanto Corporation for running the differential scanning calorimeter study and Mr. W. F. Paton for calculation of the interproton distances used for the second moment. J.Y.C. acknowledges the support of NIH Research Grant No. R01NS10903 from National Institute of Neurological Diseases and Stroke. We also wish to thank Dr. E. R. Corey for helpful discussions and the McDonnell Douglas Astronautics Co. for the use of a storage oscilloscope.

References and Notes

(1) For a review of this technique, see L. M. Jackman and F. A. Cotton, Ed., "Dynamic Nuclear Magnetic Resonance Spectroscopy", Academic Press, New York, N.Y., 1975. There are other NMR techniques that have been used in some cases to study these processes, such as spin echo, relaxation in the rotating frame, wiggle decay, and saturation transfer.
(2) W. F. Paton, J. P. Paton, J. Y. Corey, and E. R. Corey, Abstracts, 170th National Meeting of the American Chemical Society, Chicago, Ill., Aug. 1975, No. INOR-61.
(3) A. D. Hardy and F. R. Ahmed, *Acta Crystallogr., Sect. B*, **30**, 1674 (1974).
(4) A. D. Hardy and F. R. Ahmed, *Acta Crystallogr., Sect. B*, **30**, 1670 (1974).
(5) R. R. Fraser, M. H. Raza, R. N. Renaud, and R. B. Layton, *Can. J. Chem.*, **53**, 167 (1975).
(6) T. C. Farrar and E. D. Becker, "Pulse and Fourier Transform NMR", Academic Press, New York, N.Y., 1971.
(7) J. Jeener and P. Broekaert, *Phys. Rev.*, **157**, 232 (1967).
(8) A. Abragam, "The Principles of Nuclear Magnetism", Clarendon Press, Oxford, England, 1961, p 106.
(9) J. G. Powles and J. H. Strange, *Proc. Phys. Soc., London*, **82**, 6 (1963).
(10) P. Mansfield, *Phys. Rev.*, **137**, A961 (1965).
(11) N. Bloembergen, E. M. Purcell, and R. V. Pound, *Phys. Rev.*, **73**, 679 (1948).
(12) G. P. Jones, *Phys. Rev.*, **148**, 332 (1966).
(13) D. C. Ailion, *Adv. Magn. Reson.*, **5**, 177 (1971).
(14) D. C. Ailion and C. P. Slichter, *Phys. Rev.*, **135**, 1099 (1964); **137**, 235 (1965).
(15) O. Lauer, D. Stehlik, and K. H. Hausser, *J. Magn. Reson.*, **6**, 524 (1972).
(16) H. S. Gutowsky and G. E. Pake, *J. Chem. Phys.*, **18**, 162 (1950).
(17) E. R. Andrew and G. J. Jenks, *Proc. Phys. Soc.*, **80**, 663 (1962).
(18) The position of the $T_{1\rho}$ minimum depends upon the strength of the rf field H_1 (see eq 12).
(19) The position of the T_1 minimum depends upon the strength of the strong field H_1 (see eq 12).
(20) L. C. Hebel, *Solid State Phys.*, **15**, 409 (1963).
(21) D. C. Douglass and G. P. Jones, *J. Chem. Phys.*, **45**, 956 (1966).
(22) It should be noted that this range is expected to be even larger in favorable cases.
(23) H. K. Yuen, unpublished results.
(24) R. Van Steenwinkel, *Z. Naturforsch., A*, **24**, 1526 (1969).
(25) J. H. Van Vleck, *Phys. Rev.*, **74**, 1168 (1948).
(26) G. W. Smith, *J. Chem. Phys.*, **42**, 4229 (1965).
(27) J. G. Powles and H. S. Gutowsky, *J. Chem. Phys.*, **21**, 1704 (1953).
(28) D. W. Larsen and T. A. Smentkowski, results to be published.
(29) J. M. Chezeau, J. Dufourcq, and J. H. Strange, *Mol. Phys.*, **20**, 305 (1971).
(30) E. A. Andrew and R. G. Eades, *Proc. Phys. Soc., London, Sect. A*, **216**, 398 (1953).
(31) J. M. Lehn and J. Wagner, *J. Chem. Soc. D*, 414 (1970); *Tetrahedron*, **26**, 4227 (1970).
(32) A. T. Bottini and J. D. Roberts, *J. Am. Chem. Soc.*, **80**, 5203 (1958).
(33) J. Stackhouse, R. D. Baechler, and K. Mislow, *Tetrahedron Lett.*, 3437 (1971).
(34) I. J. Ferguson, A. R. Katritzky, and D. M. Read, *Chem. Commun.*, 255 (1975).
(35) F. A. L. Anet, I. Yarari, I. J. Ferguson, A. R. Katritzky, M. Moreno-Manas, and M. J. T. Robinson, *Chem. Commun.*, 399 (1976).
(36) See, for example: M. Polak and M. Sheinblatt, *J. Magn. Reson.*, **12**, 261 (1973), in which an activation barrier >6 kcal/mol for methyl reorientation is reported.

Nuclear Magnetic Resonance in Pulse Radiolysis. 2. CIDNP in Radiolysis of Aqueous Solutions[1,2]

A. D. Trifunac* and D. J. Nelson[3]

Contribution from the Chemistry Division, Argonne National Laboratory, Argonne, Illinois 60439. *Received August 10, 1976*

Abstract: Applications of magnetic resonance to the study of radiolysis are illustrated. The products of radiolytically produced radicals exhibit CIDNP when examined, seconds after their creation, by NMR. Irradiation with a pulsed electron beam (3 MeV) was carried out in variable magnetic fields and the irradiated solutions were transferred to the NMR sample tube using a fast flow system. Aqueous solutions of methanol, iodomethane, ethylene glycol, acetate, and chloroacetate were studied. In these systems CIDNP in numerous products and starting materials can be observed. The "primary radicals" of radiolysis e_{aq}^- and H play a significant role in the polarization pathways. Applicability of the radical pair model of CIDNP to radiation chemistry is illustrated.

In radiolysis when dilute aqueous solutions are irradiated practically all the energy absorbed is deposited in water molecules and the observed chemical changes are brought about indirectly via the radical products.[4] The primary radicals produced in water radiolysis are OH, e_{aq}^-, and H. These radicals react with themselves and with solutes dissolved in water. In this work we will be primarily concerned with radicals produced by OH abstraction from organic alcohols and acids and by the e_{aq}^- dissociative electron capture in alkyl halides. Both primary and secondary radicals in pulse radiolysis have been studied using several methods; the fast optical detection and electron paramagnetic resonance (EPR) are two such techniques.[4]

For some time now, we have been interested in applications of magnetic resonance to the study of pulse radiolysis, especially in the various manifestations of the chemically induced magnetic polarization phenomena. The observation of nonequilibrium electron spin populations in radicals, the so-called chemically induced dynamic electron polarization (CIDEP), in the microsecond domain[5,6] and the observation of the re-